Black rice bran-derived anthocyanins attenuate cholangiocarcinoma cell migration via the alteration of epithelial-mesenchymal transition and sialylation

SASIKAMON KHOPHAI[1], SUWADEE CHOCKCHAISIRI[2], KRAJANG TALABNIN[3], JAMES R. KETUDAT CAIRNS[1] and CHUTIMA TALABNIN[1]

[1]School of Chemistry, Institute of Science, Suranaree University of Technology, Nakhon Ratchasima 30000, Thailand; [2]College of Allied Health Sciences, Suan Sunandha Rajabhat University, Samut Songkhram 75000, Thailand; [3]School of Pathology, Institute of Medicine, Suranaree University of Technology, Nakhon Ratchasima 30000, Thailand

Received July 23, 2024; Accepted November 4, 2024

DOI: 10.3892/br.2024.1906

Abstract. Cholangiocarcinoma (CCA) is an aggressive cancer of the bile duct epithelium. Anthocyanins are water-soluble flavonoids that contribute to the color of fruits and pigmented rice. Black rice bran is rich in anthocyanin pigments and exhibits certain health benefits, including anticancer activity; however, the effect of black rice bran-derived anthocyanins (BBR-M-10) on CCA progression remains unclear. The present study assessed the cytotoxic effects of BBR-M-10 using a Sulforhodamine B assay. The metastatic properties of BBR-M-10 on CCA cell lines were investigated using wound healing, Transwell *in vitro* migration and invasion assays. The underlying mechanisms of BBR-M-10 bioactivity were examined by quantitative PCR and western blotting. Glycosylation changes were determined by lectin cytochemistry and flow cytometry. The present study demonstrated that BBR-M-10 was not toxic to CCA cell lines, but BBR-M-10 attenuated CCA cell migration and invasion, as evidenced by the increased expression levels of epithelial markers (F-actin and claudin-1), decreased expression levels of mesenchymal markers (vimentin) and a decrease in the activation and phosphorylation of AKT in BBR-M-10-treated CCA cell lines. In addition, aberrant glycosylation was observed in BBR-M-10-treated CCA cell lines, as evidenced by the low expression level of surface Sambucus Nigra lectin-binding α2,6-sialylated glycans and the reduction of α2,6 sialyltransferase gene expression levels after BBR-M-10 treatment in CCA cell lines. These findings suggested that black rice bran-derived anthocyanins could potentially be used as anti-metastatic agents against CCA.

Correspondence to: Dr Chutima Talabnin, School of Chemistry, Institute of Science, Suranaree University of Technology, 111 University Road, Suranaree, Muang, Nakhon Ratchasima 30000, Thailand
E-mail: chutima.sub@sut.ac.th

Key words: anthocyanins, cancer metastasis, epithelial-mesenchymal transition, AKT signaling pathway, sialylation

Introduction

Rice is a staple food source consumed by >50% of the global population, particularly in Asia. The demand for rice has been predicted to continue to increase in the coming decades, driven by global population growth. The rice production industry is expected to maintain its sustainability efforts and continue the production of nutraceutical by-products (1). Rice bran is a by-product of rice milling and a valuable source of nutrients containing various active phytochemicals, such as anthocyanins, tocopherols, tocotrienols, oryzanols and vitamins (1). Several studies have reported that active phytochemicals from rice bran have beneficial health effects, including antioxidant and antibacterial properties and cancer chemoprevention (2,3).

Anthocyanins are water-soluble flavonoids found in certain blue- and purple-colored vegetables, fruits and grains (4). Cyanidin-3-glycosides (C3G) and peonidin-3-glycosides (P3G) are the most abundant anthocyanins found in nature (5). Anthocyanins have been reported to effectively protect and suppress chronic diseases such as cancer, owing to their antioxidant and anti-inflammatory properties (4,6). Our previous study demonstrated that black rice bran-derived anthocyanins reduced DNA damage in H_2O_2-induced cell death in a cholangiocyte cell line via the activation of the nuclear factor erythroid 2-related factor 2-NAD(P)H quinone dehydrogenase 1 axis (7). Additionally, the anticancer effects of anthocyanins have been reported as occurring through various mechanisms, including anti-angiogenesis (8), anti-proliferation (9) and anti-metastasis (10). C3G inhibits gastric cancer proliferation and induces apoptosis through AKT/MAPK pathway inhibition (11). Cohort studies have shown that regular consumption of fruits and vegetables rich in anthocyanins is associated with a decreased incidence of colorectal (12), bladder (13) and gastric cancers (14).

Cholangiocarcinoma (CCA) is the second most common form of primary liver cancer with a high incidence in Southeast Asia, particularly in Thailand and China where liver fluke

infection is prevalent (15). CCA originates from epithelial bile duct cells and can be caused by chronic inflammation induced by *Opisthorchis viverrini* liver fluke infection (16). CCA is an aggressive type of cancer with high invasiveness, leading to poor overall patient prognosis (17). Most patients are diagnosed with advanced or metastatic CCA because CCA has non-specific symptoms during the early stages of disease (16). CCA predominantly metastasizes to the liver, lungs and lymph nodes (18). Previous studies have reported that cyanidin- and delphinidin-rich extracts from mixed plants exhibit anti-inflammatory, anti-periductal fibrosis and anti-cancer effects in *Opisthorchis viverrini*-infected hamsters and cell models (19,20). However, little is known about the inhibitory effects of black rice bran-derived anthocyanins on CCA progression. The present study aimed to investigate the effects of black rice bran-derived anthocyanins on CCA cell migration and invasion, as well as their underlying mechanisms of action, in CCA cell lines.

Materials and methods

Chemical and Reagents. Cyanidin chloride (cat. no. 80022), peonidin chloride (cat. no. 80085), cyanidin-3-glucoside (C3G; cat. no. 89616) and peonidin-3-glucoside (P3G; cat. no. 89754) were purchased from PhytoLab GmbH & Co. Sulforhodamine B (SRB; cat. no. S1402) and trichloroacetic acid (TCA; cat. no. T0699) were purchased from Sigma-Aldrich (Merck KGaA). TRIzol™ reagent (cat. no. 15596026) and the BCA Protein Assay Kit (cat. no. 23225) were obtained from Thermo Fisher Scientific, Inc. SensiFAST cDNA Synthesis Kit (cat. no. BIO-65053) was purchased from Bioline. LightCycler® 480 SYBR Green I Master Mix (cat. no. 04707516001) was purchased from Roche Diagnostics. Cell culture reagents, including DMEM (cat. no. 12100-046), Eagle's minimum essential medium (MEM; cat. no. 61100-061), penicillin-streptomycin (cat. no. 15140-122) and FBS (cat. no. 10270-098), were purchased from Gibco (Thermo Fisher Scientific, Inc.). Primary antibodies against phosphorylated AKT (pAKT; cat. no. 4060S) and total AKT (cat. no. 4685S) were purchased from Cell Signaling Technology Inc. Anti-claudin-1 (cat. no. sc-81796), vimentin (cat. no. sc-6260), slugs (cat. no. sc-166476) and β-actin (cat. no. sc-47778) antibodies were purchased from Santa Cruz Biotechnology, Inc. HRP-conjugated anti-mouse (cat. no. NXA931V) and anti-rabbit (cat. no. NA934V) secondary antibodies, ECL prime blocking reagent (cat. no. RPN415V) and ECL prime western blot detection (cat. no. RPN2236) were obtained from Cytiva. HRP-conjugated anti-goat secondary antibodies (cat. no. A15999) were purchased from Invitrogen (Thermo Fisher Scientific, Inc.). A total of 16 biotinylated lectins and ABC-peroxidase solution (cat. no. PK-4000) were purchased from Vector Laboratories, Inc. (Maravai LifeSciences). The SignalStain® DAB substrate kit (cat. no. 8059) was obtained from Cell Signaling Technology, Inc. Alexa fluor 488 conjugated streptavidin (cat. no. S11223; 1:400) was purchased from Thermo Fisher Scientific, Inc.

BBR-M-10 preparation. Black rice bran from black-pigmented rice (*Oryza sativa* L.) was collected from a rice mill in Krabueang Yai (Nakhon Ratchasima, Thailand). The black rice bran extract enriched in anthocyanins was prepared as previously described (7). Briefly, black rice bran was soaked in n-hexane followed by 0.1% HCl in MeOH at room temperature for 24 h. The MeOH extracts were filtered and evaporated to obtain powdered extracts. The powder extracts were subjected to silica column chromatography (CC) using a gradient solvent system of hexane [hexane-ethylacetate (EtOAc), EtOAc, EtOAc-MeOH and MeOH]. A total of eight fractions were obtained, and the anthocyanin contents were investigated via thin-layer chromatography (TLC) and compared with the cyanidin, peonidin, C3G and P3G standards. Fractions with high contents of C3G and P3G via TLC were further purified using Sephadex LH20 CC in MeOH:H_2O (80:20) to produce fractions. A total of four fractions, including BBR-M-10 from Sephadex LH20 CC were analyzed via TLC. TLC analysis demonstrated that the main anthocyanin components in BBR-M-10 were C3G and P3G when compared with the standard compounds. Anthocyanin content was further analyzed using high-performance liquid chromatography and compared with the cyanidin, peonidin, C3G and P3G standards. HPLC analyses were performed using the 1260 Infinity instrument (Agilent Technologies, Inc.) The separation of anthocyanins was analyzed using a ZORBAX SB-C18 StableBond Analytical 4.6x250 mm 3.5 μM column. The mobile phases used were: A, 0.1% TFA in deionized water and B, acetonitrile. The gradient conditions were as follows: B at 10% for 5 min, followed by a linear increase to 15% B over the following 15 min, a hold at 15% B for 5 min, then an increase in B from 15-18% over 5 min followed, by 18-35% B over 20 min, then B at 35-90% for 10 min. The detection wavelength was 520 nm. The chromatographic conditions were as follows: Flow rate, 1 ml/min; column temperature, 35˚C; 20 μl injection; stop time, 60 min; and post time, 10 min. The total anthocyanin content of BBR-M-10 was 108 mg CGE/100 g DW (100 mg/l). BBR-M-10 comprises C3G (94.5 mg/l) and P3G (2.47 mg/l).

Cell culture. Human CCA cell lines (KKU-055 and KKU-213A), a normal human lung fibroblast line (IMR-90) and an immortalized human cholangiocyte (MMNK-1) cell line were used. KKU-055 (cat. no. JCRB1551) and KKU-213A (cat. no. JCRB1557) were previously established and authenticated (21). Certificates of analysis were obtained from the Japanese Collection of Research Bioresources Cell Bank. The immortalized human cholangiocyte MMNK-1 cell line was provided by Dr. Sopit Wongkham (Khon Kaen University, Thailand). CCA cell lines and MMNK-1 were cultured in DMEM supplemented with inactivated 10% FBS and 100 U/ml penicillin-streptomycin. IMR-90 cells (cat. no. CCL-186) were obtained from the American Type Culture Collection and cultured in EMEM supplemented with inactivated 10% FBS and 100 U/ml penicillin-streptomycin. All the cell lines were incubated at 37˚C in a humidified incubator containing 5% CO_2. PCR assays were used to verify the lack of mycoplasma contamination in all cell lines.

BBR-M-10 treatment and cell viability. KKU-055, KKU-213A, IMR-90 and MMNK-1 cells were seeded at $7x10^3$ cells/well into 96-well plates and incubated overnight. The cells were then treated with various concentrations of BBR-M-10 from 0-5,000 μg/ml and incubated for 24 h. Cell viability was

Table I. Primer sequences used for quantitative PCR.

Gene	Sequence (5'-3')
ST3GAL1	F: GGACCCTGAAAGTGCTCA
	R: TCTCCAGCATAGGGTCCA
ST3GAL3	F: GTATGATCGGTTGGGCTTC
	R: CGCTCGTACTGCTCAGG
ST3GAL4	F: GTCAGCAAGTCCCGCT
	R: CTTGTTGATGGCATCTCCC
ST3GAL6	F: GGTATCTTGTGGCCATATTCC
	R: CTCCATTACCAACCACCAC
ST6 β-galactoside α-2,6-sialyltransferase 1	F: CTTGTTTTCCTGCTCAGA
	R: GCAAACAGAAGAAAGACCA
β-actin	F: GATCAGCAAGCAGGAGTATGACG
	R: AAGGGTGTAACGCAACTAAGTCATAG

ST3Gal, ST3 β-Galactoside α-2,3-Sialyltransferase; F, forward; R, reverse.

assessed using the SRB assay. Briefly, treated cells were fixed with 10% TCA at 4˚C for overnight and stained with 0.4% (w/v) SRB in 1% (v/v) acetic acid at room temperature for 30 min. The unbound SRB was removed, washed three times with 1% (v/v) acetic acid and dried. Next, the stained cells were solubilized in 10 mM Tris-base (pH 10) and mixed in a shaker at room temperature for 15 min. Absorbance at 564 nm was measured using a TECAN Infinite 200 Pro microplate reader (Tecan Group, Ltd.). The IC_{50} was calculated using GraphPad Prism (version 8; Dotmatics).

RNA extraction and quantitative PCR. KKU-055 and KKU-213A cells were seeded at $3.5x10^5$ cells/well into 6-well plates. After 24 h, cells were treated with BBR-M-10 at 0 and 200 μg/ml for 24 h. Total RNA was extracted using TRIzol™ reagent according to the manufacturer's instructions. RNA quantity and quality were measured using a NanoDrop 2000 spectrophotometer (NanoDrop Technologies; Thermo Fisher Scientific, Inc.) and agarose gel electrophoresis, respectively. A SensiFAST cDNA Synthesis Kit was used to synthesize cDNA. Quantitative PCR was performed using the LightCycler® 480 SYBR Green I Master Mix to investigate gene expression. The primer sequences for all genes were obtained from previous studies (Table I) (22,23). Gene amplification was performed by initial denaturation at 95˚C for 5 min, followed by 40 cycles of denaturation at 95˚C for 10 sec, annealing at 50˚C for ST6GAL1, annealing at 60˚C for ST3GAL1, 3, 4, and 6 for 10 sec and a final extension at 72˚C for 10 sec. b-actin was used as the endogenous control. The relative mRNA levels of each gene were normalized to b-actin and calculated using the $2^{-\Delta\Delta Cq}$ method (24).

Wound-healing assay. KKU-055 and KKU-213A cells were seeded at a density of $3x10^5$ cells/well in 24-well plates. After 24 h of growth to 90% cell confluence, a vertical wound was scratched through the cell monolayer using a sterile 200 μl plastic micropipette tip. Cell debris was removed and replaced with BBR-M-10 at 50, 100 and 200 μg/ml in serum-free DMEM. Cell migration during the wound healing process was observed and digitally photographed using a light microscope at 0, 12, 18 and 24 h (magnification, x100). The wound area was evaluated using Image J software (version 1.53a; National Institutes of Health) and calculated as follows: (Area of original wound-area of wound during healing)/area of the original wound.

Transwell migration and invasion assay. Transwell inserts were coated with 100 μl of Matrigel 200 μg/ml and incubated at 37˚C for 2 h. KKU-055 and KKU-213A cells at a density of $1x10^5$ cells in 200 μl of FBS-free medium with or without BBR-M-10 at 50, 100 and 200 μg/ml were seeded into Transwell inserts for the migration assay Matrigel-coated Transwell inserts for the invasion assay. Next, 600 μl of 10% FBS-containing medium was loaded into the lower chamber to create a chemotactic gradient and incubated at 37˚C. After 12 h, the Transwell inserts were removed from the plate and a cotton-tipped applicator was used to remove the cells on the upper side of the membranes. The migrated cells on the bottom side of the membranes were fixed with 10% TCA at 4˚C overnight, stained with SRB at room temperature for 30 min, washed with 10% acetic acid and dried. Images of migrated cells were captured using a light microscope and counted. Migrated cells were counted in five fields of view. The presented values were the number of total migrated cells per fields of view at x100 magnification.

Lectin cytochemistry. KKU-055 and KKU-213A cells were seeded at a density of $3x10^4$ cells/well in 24-well plates and incubated overnight. The cells were treated with 0 and 200 μg/ml BBR-M-10 for 24 h. The cells were fixed with 4% paraformaldehyde in PBS for 15 min and permeabilized with 0.1% Triton X-100 in PBST for 10 min at room temperature. The endogenous hydrogen peroxide-generating activity was blocked with 0.3% hydrogen peroxide for 30 min at room temperature. Nonspecific binding was blocked with 3% BSA (HIMedia Laboratories, LLC) for 30 min at

Table II. Glycan expression in CCA cell lines evaluated by staining with a panel of 16 lectins.

		KKU-055		KKU-213A	
Lectin	Major sugar	0 μg/ml	200 μg/ml	0 μg/ml	200 μg/ml
Arachis hypogaea (peanut) agglutinin	Galactose	++	++	+	+
Glycine max (soybean)	N-acetylgalactosamine	+	+	+	+
Ulex europaeus agglutinin I;	Fucose	++	++	+++	++
Triticum vulgaris (wheat germ)	N-acetylglucosamine	+++	+++	+++	+++
Dolichos biflorus agglutinin	N-acetylgalactosamine	+++	+++	+++	+++
Ricinus communis agglutinin	N-acetylgalactosamine	+++	+++	+++	++
Concanavalin A	Mannose	+++	+++	+++	+++
Lycopersicon esculentum (tomato) lectin	N-acetylglucosamine	+++	+++	++	++
Erythrina cristagalli lectin	Galactose	+++	+++	+++	+++
Solanum tuberosum (potato) lectin	N-acetylglucosamine	+	+	+	+
Jacalin	Galactose	+	+	+	+
Datura Stramonium lectin	N-acetylglucosamine	++	++	++	++
Vicia villosa agglutinin	N-acetylgalactosamine	+	+	++	++
Griffonia (*Bandeiraea*) *simplicifolia* lectin II	N-acetylglucosamine	++	++	++	++
Sambucus nigra lectin	(α2,6) linked sialic acid	+++	+++	+++	++
Maackia Amurensis lectin II	(α2,3) linked sialic acid	-	-	+	+

+++, strong expression; ++ moderate expression; + slight expression; -, no expression.

room temperature. A 1:500 dilution of biotinylated lectins (Table II) was added and incubated at 4˚C overnight on a shaker. The ABC-Peroxidase Solution was then used as the secondary antibodies for 1 h at room temperature to determine the lectin signal. A SignalStain® DAB substrate kit was used to visualize the signal under a light microscope at x100 magnification.

Lectin staining by flow cytometry. KKU-055 and KKU-213A cells were seeded at a density of $3x10^5$ cells/well in 6-well plates and incubated at 37˚C. After 24 h, the cells were treated with 0 and 200 μg/ml BBR-M-10 and incubated at 37˚C for 24 h. The cell pellet was harvested and washed with 2% FBS in PBS. The cell pellet was fixed with 4% paraformaldehyde in PBS at room temperature for 15 min and nonspecific binding was blocked with 3% BSA for 30 min on ice. The cell pellet was then incubated for 1 h on ice with biotinylated SNA lectins (cat. no. PK-4000; 1:500). Alexa fluor 488 conjugated streptavidin (cat. no. S11223; 1:400) was then added for 1 h on ice to determine the lectin signal. Cell pellets were resuspended in 2% FBS in PBS and analyzed by flow cytometry using Attune NxT fluorescent detector and Attune Cytometric Software (version 5.3.2415.0; Thermo Fisher Scientific, Inc.). Then mean fluorescence intensity was analyzed using the Flowing software (version 2; Turku Bioscience).

Immunofluorescent analysis. KKU-055 and KKU-213A cells were seeded at a density of $2.5x10^4$ cells/well in 8-well cell culture slides and incubated at 37˚C and 5% CO_2 overnight. After 24 h of incubation, cells were treated with 0 and 200 μg/ml BBR-M-10 for 24 h. The cells were washed with PBS and fixed with 4% paraformaldehyde at room temperature for 15 min. The fixed cells were permeabilized with 0.1% Triton-X100 in PBS for 10 min on ice. A blocking solution (2% BSA in 0.1% PBST) was added to the cells for 30 min on ice, and then the cells were incubated at 4˚C overnight with phalloidin Alexa Fluor 647 antibodies (cat. no. #8940S; 1:50; Cell Signaling Technology, Inc.). After washing with PBS, nuclear counterstaining with Hoechst 33258 solution (1:1,000) was performed on ice for 10 min. Stained cells were visualized using a confocal microscope (Nikon Corporation).

SDS-PAGE and western blotting analysis. KKU-055 and KKU-213A cell lysates were extracted using protein lysis buffer containing 10% TritonX, protease inhibitor cocktail (Roche diagnostics GmbH) and Tris-lysis buffer pH 7.5. The protein determination method was a BCA protein assay kit (Thermo Fisher Scientific Inc.). A total of 40 μg of protein extracts were separated using 10-15% SDS-PAGE and transferred to a nitrocellulose membrane (Cytiva). Non-specific binding was blocked with 5% ECL prime blocking reagent (Cytiva) containing 0.05% Tween 20 at room temperature for 1 h. Then, the membranes were probed with primary antibodies at dilutions of 1:1,000 for vimentin, claudin-1, pAKT and AKT and 1:500 for ST6GAL1 in 0.05% PBST at 4˚C overnight. The membranes were then washed three times with 0.1% PBST three times for 10 min each. Membranes were incubated with secondary antibodies at room temperature for 1 h. ECL™ Prime Western blotting detection reagents (Cytiva) were used to determine the target protein signals and visualized using the ImageQuant™ LAS 500 (Cytiva). The density of each target protein was determined using ImageJ software and normalized to β-actin.

Statistical analysis. The results were expressed as the mean ± SD (n=3). The one-way ANOWA followed by Bonferroni's multiple comparisons test was used to analyze data. GraphPad Prism was used for data analysis. P<0.05 was considered to indicate a statistically significant difference.

Results

Effect of BBR-M-10 on cell viability. To evaluate the effect of BBR-M-10 on CCA cell viability, KKU-055 and KKU-213A cells were treated with BBR-M-10 at various concentrations. A normal fibroblast cell line (IMR-90) was used as the normal control cell line because IMR-90 cells were derived from a human embryo with a normal karyotype and have a finite lifespan (25). The cell viability test demonstrated that BBR-M-10 was not toxic to KKU-055, KKU213A and IMR-90 cells. The respective IC_{50} value for BBR-M-10 was 2.94 and 3.47 mg/ml, for the CCA cell lines KKU-055 and KKU-213A, respectively, and for IMR-90 cells it was 4.30 mg/ml (Fig. 1A). Additionally, the effect of BBR-M-10 in MMNK-1 cells was measured. The IC_{50} value for BBR-M-10 was 0.75 mg/ml for MMNK-1 (Fig. S1). Taken together, the decreases in cell viability of MMNK-1 and CCA cell lines were observed at high doses of BBR-M-10 (1,250-5,000 μg/ml), whereas high doses of BBR-M-10 showed less toxicity to the IMR-90 cell line (Fig. S2). Our previous study demonstrated that the main anthocyanin components in BBR-M-10 are C3G and P3G (7). Thus, the effects of C3G and P3G on CCA cell viability were investigated in both CCA cell lines. These results showed that CCA cell viability was not significantly impacted by C3G or P3G treatment at 0-500 μM (Fig. 1B and C). Thus, low doses of BBR-M-10 (50, 100 and 200 μg/ml) were selected to assess the effect of BBR-M-10 on CCA cell migration and invasion.

BBR-M-10 inhibited CCA cell migration and invasion. The effects of anthocyanins on crucial cancer cell properties, including cell proliferation, migration and invasion, have been documented in various types of cancers such as squamous cell carcinoma, liver cancer, CCA and cervical cancer (10,19). To address whether BBR-M-10 affected cancer cell activity, the migration and invasion properties of CCA cell lines upon BBR-M-10 treatment were assessed using wound healing, Transwell migration and invasion assays. KKU-055 and KKU213A cells were treated with BBR-M-10 at 0, 50, 100 and 200 μg/ml. The wound healing assay results demonstrated a statistically significant dose-dependent decrease in the migration ability of both KKU-055 and KKU-213A cells (Fig. 2A and B). Additionally, BBR-M-10 treatment at 100 and 200 μg/ml significantly decreased the migration area in both KKU-055 and KKU-213A cells. Transwell migration assay results demonstrated that BBR-M-10 treatment at 50, 100 and 200 μg/ml significantly reduced the migration ability of KKU-055 and KKU-213A cells (Fig. 3A and B). Moreover, BBR-M-10 treatment at 200 μg/ml significantly decreased the cell invasion ability of KKU-055 and KKU-213A cells (Fig. 3C). These findings suggested that BBR-M-10 may inhibit the signaling pathway that promotes CCA cell migration and invasion.

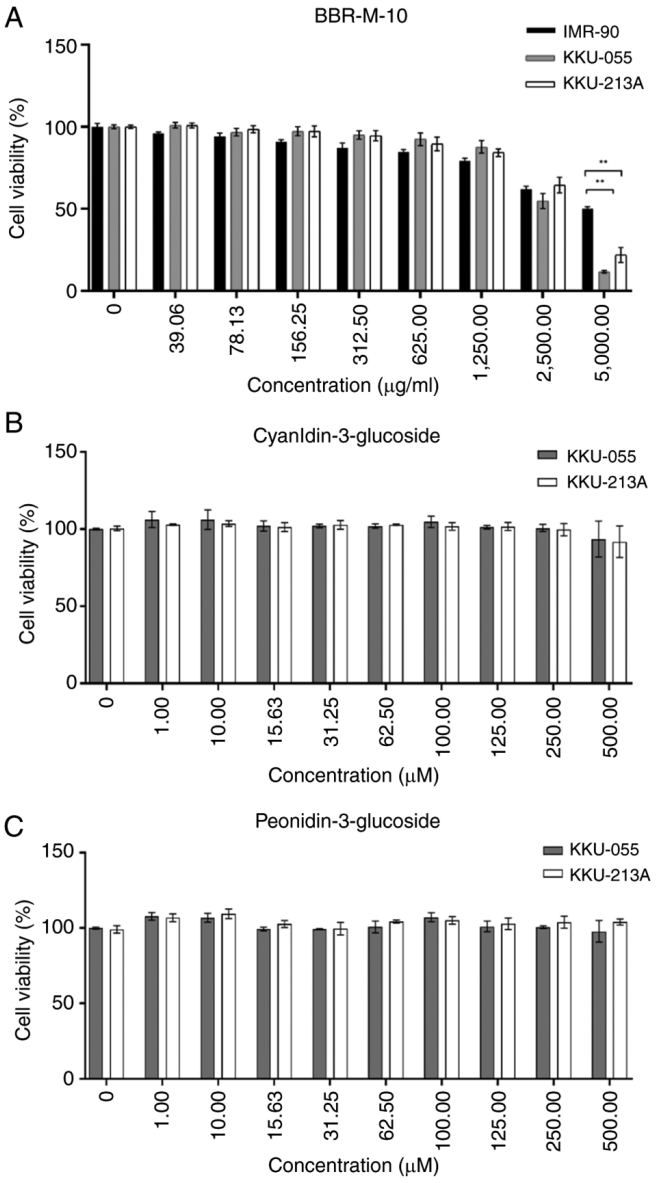


Figure 1. Anti-proliferative effect of BBR-M-10 on CCA cell lines. (A) BBR-M-10 treatment at concentration 0, 39.06, 78.13, 156.25, 312.50, 625.00, 1,250.00, 2,500.00 and 5,000.00 μg/ml in CCA cell lines and normal lung fibroblasts (IMR-90). (B) Cyanidin-3-glucoside and (C) peonidin-3-glucoside treatment at concentration 0, 1,10, 15.63, 31.25, 62.50, 100, 125, 250, and 500 μM in CCA cell lines. Data were presented as mean ± SD (n=3). **P<0.01. CCA, cholangiocarcinoma.

BBR-M-10 attenuated epithelial-mesenchymal transition in CCA via the AKT pathway. Actin polymerization serves a crucial role in regulating cell structure during cancer cell migration and invasion (26). To address the effect of BBR-M-10 on lamellipodium formation, KKU-055 and KKU213A cells were treated with BBR-M-10 at 0, 100 and 200 μg/ml. The distribution of filamentous actin (F-actin) and the overall shape of cells were detected by phalloidin staining and visualized using confocal microscopy. BBR-M-10 reduced F-actin accumulation at the edges of both KKU055 and KKU-213 cells, suggesting a decrease in migration ability (Fig. 4A). Epithelial-to-mesenchymal transition (EMT) is a crucial initiating step in cancer invasion and metastasis and is modulated via multiple signaling pathways, including

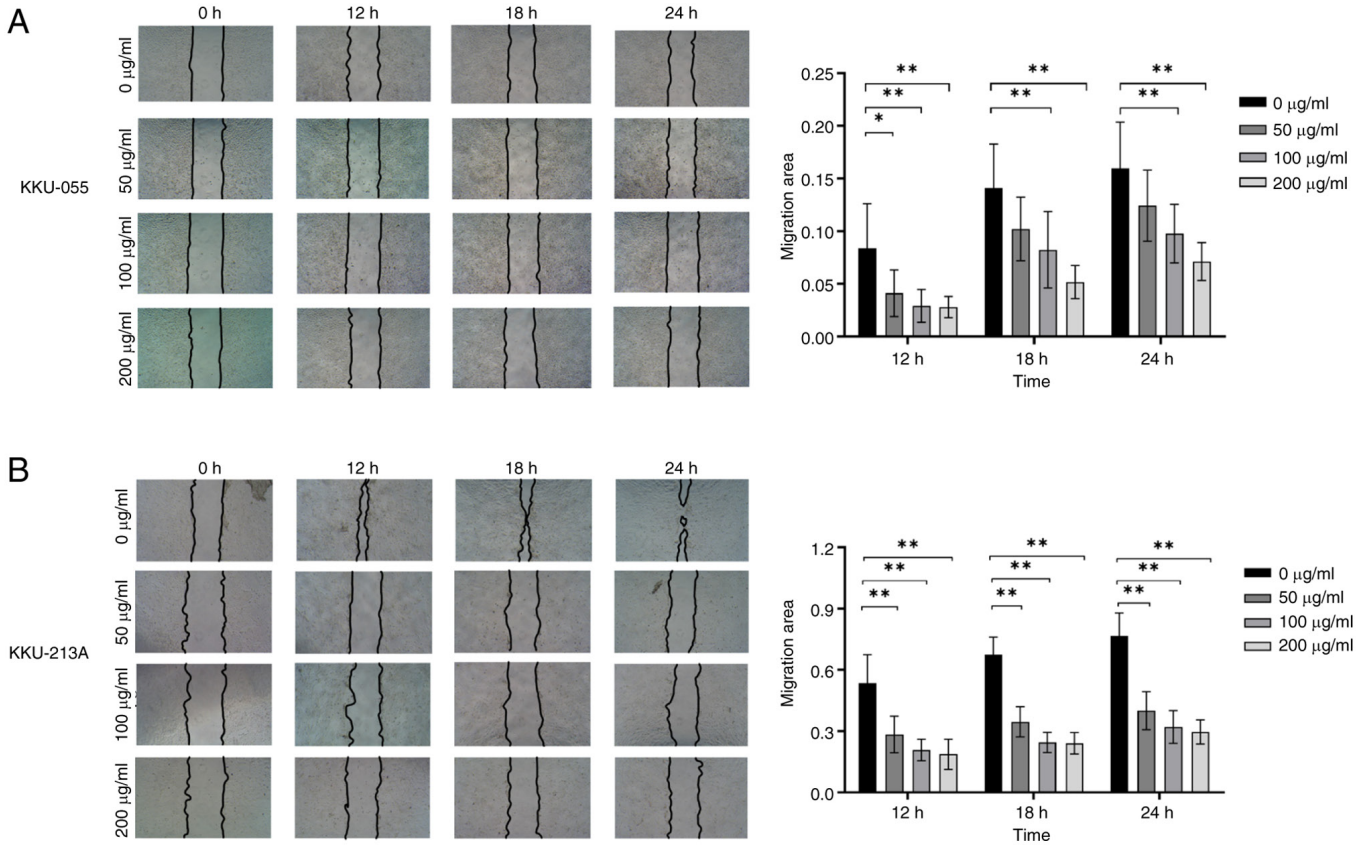


Figure 2. Effect of BBR-M-10 on migration of cholangiocarcinoma cell lines. A wound healing assay was performed to evaluate the migration of (A) KKU-055 and (B) KKU-cell lines upon BBR-M-10 treatment at 50, 100 and 200 μg/ml for 0, 12, 18 and 24 h after wounding. Magnification, x200. Data were presented as mean ± SD (n=3). *P<0.05, **P<0.01.

AKT signaling. Several EMT markers, including claudin-1, Slug and vimentin, are regulated by this pathway (27). The effect of BBR-M-10 on CCA cell migration and invasion via EMT was also investigated. Western blotting analysis demonstrated that BBR-M-10 treatment at 100 and 200 μg/ml markedly increased the protein expression levels of expression of claudin-1 in KKU-055 (Fig. 4B). BBR-M-10 treatment at 200 μg/ml significantly decreased vimentin protein expression levels compared with cells treated with 100 μg/ml BBR-M-10. Additionally, a marked reduction in the ratio of phosphorylated to non-phosphorylated AKT (pAKT/AKT) was observed in KKU-055 cells treated with BBR-M-10 at 100 and 200 μg/ml. The protein expression levels of claudin-1 were markedly increased, whilst the protein expression levels of vimentin were markedly decreased in KKU-213A cells treated with 100 and 200 μg/ml BBR-M-10 (Fig. 4B). A marked decrease in the pAKT/AKT ratio was observed in KKU-213A cells treated with BBR-M-10 at 200 μg/ml only.

BBR-M-10 altered sialylation in CCA. Aberrant glycosylation is a hallmark of cancer and is associated with certain behaviors exhibited by cancer cells, including EMT (28). To investigate whether BBR-M-10 induced glycosylation changes in CCA cell lines, a panel of 16 lectins were used to identify differences in glycan expression between BBR-M-10-treated and control CCA cells (Table II). Lectin cytochemistry demonstrated that low expression levels of SNA binding α2,6-sialylated glycan was observed in BBR-M-10-treated KKU-213A cells compared with the control (Fig. 5A). Additionally, flow cytometry analysis confirmed that surface SNA binding α2,6-sialylated glycan showed a significant decrease in expression levels in BBR-M-10-treated KKU-213 cells (Fig. 5B). Next, it was further investigated whether BBR-M-10 altered the expression of sialyltransferase genes, including α2,3 sialyltransferase genes *ST3GAL1*, 2, 3, 4 and 6 and α2,6 sialyltransferase gene *ST6GAL1*. Gene expression level analysis demonstrated that the mRNA expression levels of *ST3GAL4 and ST6GAL1* were significantly reduced after BBR-M-10 treatment in KKU-213 cells compared with the control cells (Fig. 5C).

Moreover, the protein expression level of ST6GAL1 was significantly decreased after BBR-M-10 treatment in KKU-213 cells (Fig. 5D). The altered expression of α2,3-sialylated glycans in both CCA cell lines was not detected via MAL II Lectin staining after BBR-M-10 treatment. Therefore, the protein expression levels of ST3GAL4 were not included in the present study. Taken together, these findings suggest that BBR-M-10 may affect CCA progression via the reduction of glycoprotein sialylation.

Discussion

Cancer is a disease characterized by certain cellular properties, including increased proliferation, migration, invasion, metastasis and drug resistance (29). Despite the approval of various chemotherapies for cancer treatment, success in improving the survival of patients with metastatic cancer

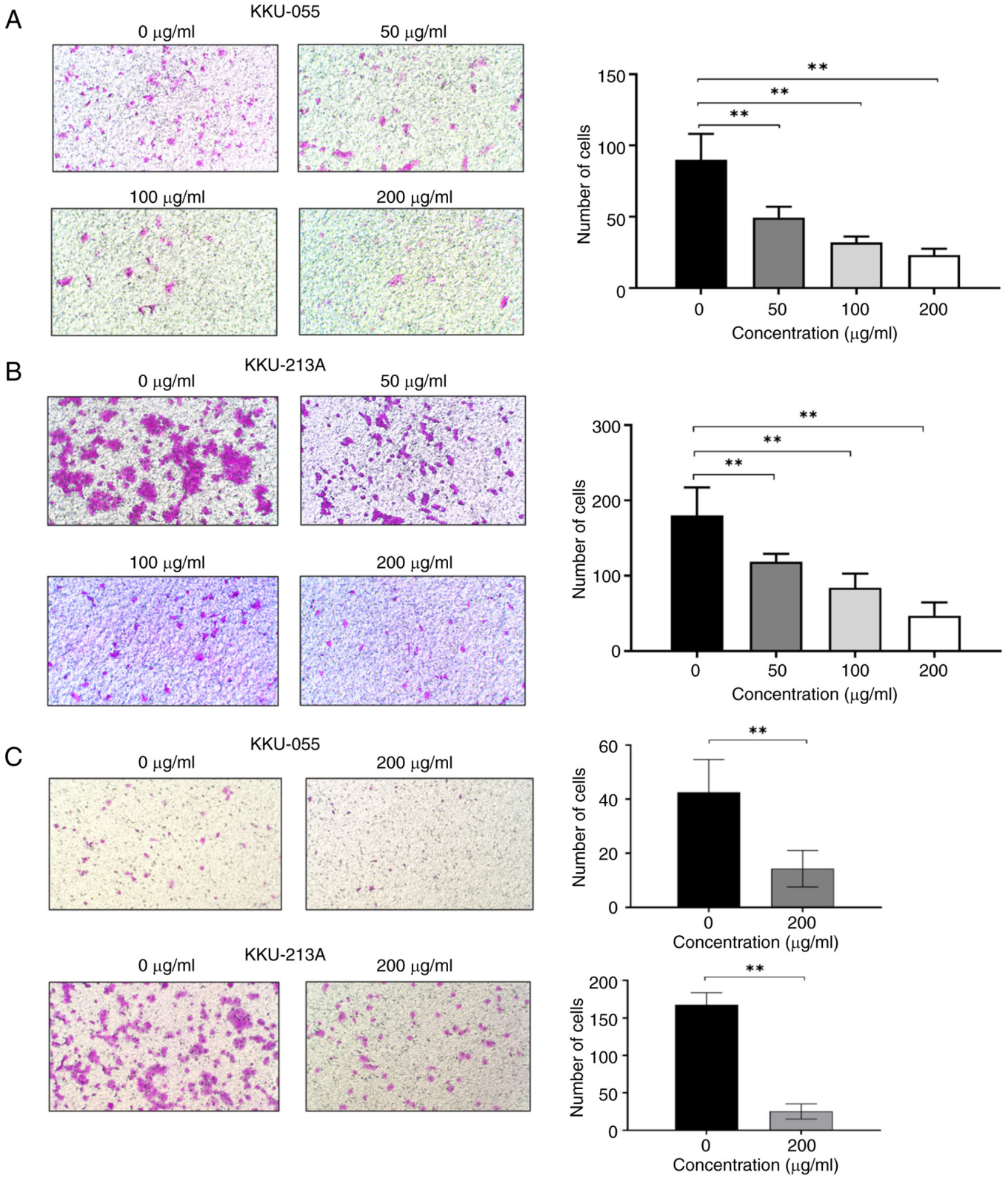


Figure 3. Effect of BBR-M-10 on Transwell migration and invasion of cholangiocarcinoma cell lines. Transwell migration assays of (A) KKU-055 and (B) KKU-2013A cells upon 0, 50, 100 and 200 μg/ml BBR-M-10 treatment were evaluated after 12 h. (C) Invasion assays were performed to evaluate the invasion of KKU-055 and KKU-213A cells upon BBR-M-10 treatment at 0 and 200 μg/ml for 12 h. Magnification, x200. Data were presented as mean ± SD (n=3). **P<0.01.

remains limited (30). In liver fluke-associated CCA, cell migration to the lymph nodes and distant metastasis are crucial factors affecting poor prognosis and shortened survival in patients with CCA (31,32). Therefore, appropriate therapeutic drugs are needed to prevent and treat CCA. The present study focused on the potential role of BBR-M-10 in reducing CCA progression. These results demonstrated that BBR-M-10 did not cause significant cytotoxic effects in

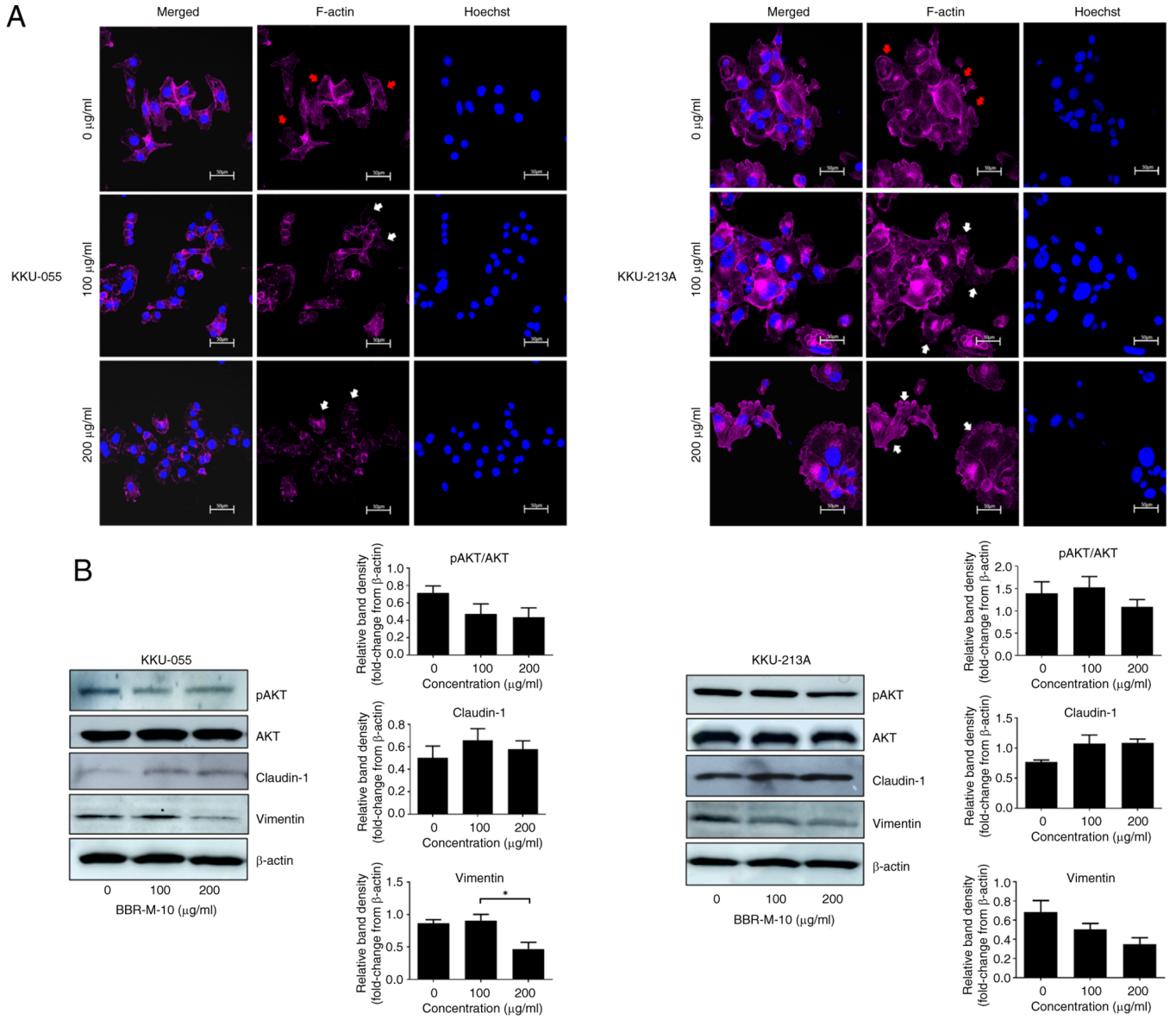


Figure 4. BBR-M-10 reduces the accumulation of actin filament and epithelial-mesenchymal transition via the AKT pathway. KKU-055 cells and KKU-213A cells were treated with BBR-M-10 at 0, 100 and 200 μg/ml for 24 h. (A) Detection of F-actin was performed with Phalloidin staining. Red arrows indicated positive F-actin staining, whereas white arrows indicated weak staining of F-actin. Scale bar, 50 μm. (B) Western blotting analysis of pAKT, AKT, Claudin-1, and Vimentin expression in KKU-055 and KKU-213A cells. Data were presented as mean ± SD (n=3). *P<0.05. P, phosphorylated.

either CCA cell lines or normal cells. This result is consistent with previous studies on hepatocellular carcinoma, breast cancer and prostate cancer (10,33,34). The cytotoxicity of BBR-M-10 in the immortal MMNK-1 cholangiocyte cell line was also performed. A decrease in the viability of MMNK-1 and CCA cells was observed at high doses of BBR-M-10, whereas high doses of BBR-M-10 were less toxic to IMR-90 cells. This may be due to the immortality of MMNK-1 with retroviral vector encoding simian virus 40 large T and human telomerase, whereas IMR-90 cells are derived from a human embryo with a normal karyotype and have a finite lifespan (25,35). Thus, IMR-90 cells were selected as the control cell line in the present study instead of MMNK-1 cells, because they are a human-derived cell line and are well characterized. Additionally, IMR-90 cells have not undergone genetic modifications that could affect their behavior.

Intuyod *et al* (20) anthocyanin complex (AC) nanoparticles serve a role in CCA development and progression, as evidenced by anti-inflammatory and anti-fibrotic effects of AC nanoparticles in an *O. viverrini*-infected hamster model and the anticancer activity of AC nanoparticle in CCA cell lines. BBR-M-10 exhibits a chemoprotective effect on CCA via the reduction of reactive oxygen species and the anti-metastatic effect of BBR-M-10 in CCA cell lines has been previously reported (7). Anthocyanins exhibit a wide variety of biological activities. This may be due to the types of anthocyanins in the extract used. BBR-M-10 is composed of C3G and P3G, whereas the AC nanoparticles were prepared from cyanidin, delphinidin, turmeric extract, caffeic acid and piperine. Intuyod *et al* showed that AC nanoparticles mainly had an effect on CCA cell death. This may be due to the growth inhibition caused by delphinidin or turmeric extract that has been previously reported in various types of cancers including

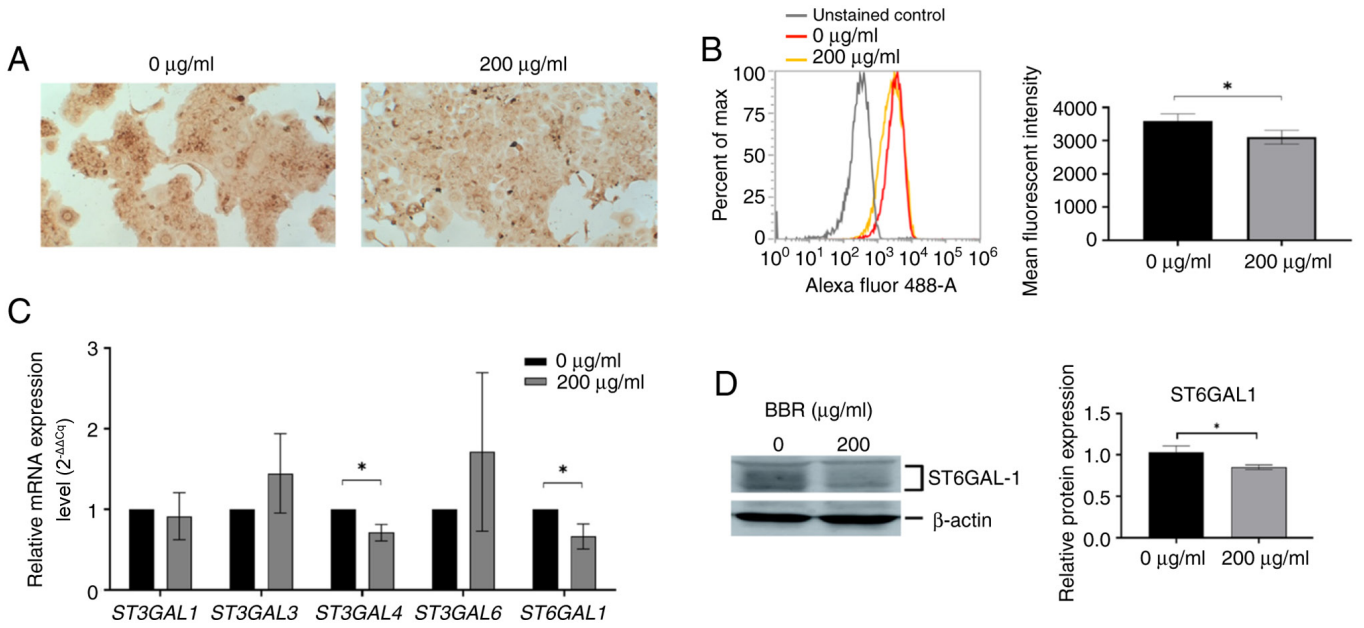


Figure 5. BBR-M-10 alters sialylation of KKU-213A cells. KKU-213A cells were treated with BBR-M-10 at 200 μg/ml for 24 h. (A) Cytochemical staining of α2,6-sialylated glycan was detected with SNA lectin in KKU-213A. (B) Intensity of α2,6-sialylated glycan was detected with SNA lectin in KKU-213A and analyzed by flow cytometry. Histogram overlays of the negative control (gray), untreated group (red) and BBR-M-10 treated group (yellow). (C) Relative mRNA expression level of sialyltransferases in BBR-M-10-treated CCA cell lines and control cells. (D) ST6GAL1 protein expression levels in BBR-M-10 treated KKU-213A. Data were presented as mean ± SD (n=3). *P<0.05.

CCA (36,37). Taken together, BBR-M-10 significantly decreased the migration and invasion of CCA cell lines via reduced lamellipodium formation and EMT. Thus, BBR-M-10 treatment might represent an alternative treatment for metastatic CCA.

EMT facilitates metastasis in various types of cancers (38,39). EMT triggers a phenotypic shift in epithelial cancer cells, transforming them into mesenchymal cells, ultimately leading to cancer cell metastasis (38). Mesenchymal cells exhibit loss of cell-to-cell interactions regulated by a decrease in epithelial cell markers and an increase in the expression of mesenchymal cell markers (40). Numerous studies have highlighted the effects of anthocyanins on cancer cell invasion. Anthocyanins derived from plants and fruits exhibit anti-metastatic effects in various cancers, including hepatocellular carcinoma and breast and prostate cancers (10,33,34). These studies are consistent with our present study, in which BBR-M-10 significantly reduced the migration and invasion of CCA cell lines (10,31,34). The actin cytoskeleton regulates cell structure and motility, allowing cells to migrate and invade (26). The dynamic polymerization and depolymerization of F-actin are regulated by actin-binding proteins, which typically stabilize the polymerization of F-actin and drive the protrusion of the cell membrane (26,41). Alteration and accumulation of F-actin at the cell edges or in the lamellipodium has been reported to contribute to the aggressiveness of cancer cell invasion through the extracellular matrix in several cancer types (42,43). The reduction in F-actin in lamellipodia formation has been associated with a decrease in cancer invasiveness (44). Previous studies reported the effects of flavonoids and anthocyanins on the disruption of F-actin formation in diabetic kidney and prostate cancer cells (34,45). In the present study, BBR-M-10 reduced F-actin accumulation in CCA cell lines. These findings suggest that BBR-M-10 prevented CCA cell migration and invasion by modulating F-actin formation.

Moreover, BBR-M-10 altered the expression of EMT genes via the upregulation of epithelial markers (claudin-1) and downregulation of mesenchymal markers (vimentin). This may be due to the role of vimentin in providing flexibility to cells and promoting cell motility in various cancers (46,47). In addition, claudin-1 is recognized as a tight junction protein. Downregulation of claudin-1 can be associated with invasion in various cancers, including CCA (40,48). However, in some cancers, claudin-1 has the opposite role in that its high expression levels suggests its potential involvement in the progression of cancers, such as colon cancer (49). The findings of the present study suggested that BBR-M-10 attenuated CCA cell migration and invasion via a decrease in the EMT.

The PI3K/AKT pathway has been reported to be a driver of cancer progression through increasing cell proliferation and metastasis (50). The increase in activation of the PI3K/AKT signaling pathway is correlated with cell growth and metastasis in CCA (51). Additionally, downregulation of epithelial marker E-cadherin, and upregulation of EMT-related transcription factors (EMT-TFs), including Snail, Twist and ZEB1 in CCA tissues were strongly associated with a positive metastasis status (52). It has been reported that EMT-TFs, including Snail, Twist and ZEB1, are regulated by the PI3K/AKT pathway. EMT-TFs induce the expression of mesenchymal markers, including N-cadherin and vimentin, and suppress the expression of epithelial markers such as E-cadherin and claudin-1 (53,54). Additionally, inhibition of AKT activity reduces the expression of EMT-TFs and EMT markers, leading to decreases in cell migration and invasion (55,56). In the present study, BBR-M-10 diminished the phosphorylation of AKT in CCA cell lines, resulting in increased

claudin-1 and decreased vimentin expression levels in CCA cell lines. This finding is consistent with studies in breast cancer, in which anthocyanins extracted from cherries reduced invasion of cells via downregulation of AKT expression (57). Additionally, MK-2206 is an orally active allosteric Akt inhibitor. The effects of MK2206 on CCA migration and invasion have been previously reported. MK2206 reduces the phosphorylation of Akt leading to the reduction of CCA migration and invasion (58). In the present study, the phosphorylation of AKT upon BBR-M-10 treatment was markedly decreased in both CCA cell lines. Additionally, Chen *et al* (59) and Zhou *et al* (33) demonstrated that black rice anthocyanins inhibit EMT and metastasis of breast cancer cells by targeting the RAS/RAF/MAPK pathway or protein tyrosine kinase 2 (FAK) signaling. Therefore, the potential anti-metastatic effect of BBR-M-10 via RAS/RAF/MAPK pathway or FAK signaling in CCA requires further study in the future.

Glycosylation, a major post-translational modification, usually acts as a fine tuner of cellular and molecular interactions (60). Glycosylation changes are a hallmark of cancer that serve a signaling role in several aspects of malignancy, including proliferation, invasion and metastasis. EMT is a critical step in metastasis and is associated with glycosylation changes, as evidenced by N-glycan branching, O-glycan truncation, terminal sialylation and terminal fucosylation during EMT (61). The present study demonstrated a decrease in terminal α2,6-sialylated glycans in CCA cell lines via SNA Lectin staining after BBR-M-10 treatment. However, BBR-M-10 altered the expression levels of sialyltransferases only in KKU-213A cells and downregulated ST6GAL1 expression, the primary enzyme responsible for α2,6sialylation. These findings suggested that BBR-M-10-altered sialylation is cell type-specific, since KKU-213A has a high invasion capacity. This is consistent with a previous study that showed that patients with metastatic CCA with low ST6GAL1 expression levels had a shorter overall survival compared with patients with metastatic CCA with high ST6GAL1 expression levels (62).

Moreover, ST6GAL1 overexpression promotes cell migration and invasion by activating the PI3K/AKT signaling pathway (63). Based on the results of the present study, it could be suggested that BBR-M-10 attenuated AKT activation, reduced CCA cell migration and invasion through the downregulation of ST6GAL1 and EMT-related genes. To the best of our knowledge, the present study was the first to report the effect of anthocyanins on cancer-associated glycosylation. However, further studies are needed to elucidate the mechanism of action underlying BBR-M-10-modulated sialylation.

In conclusion, black rice bran is a valuable source of anthocyanins with beneficial health effects. In the present study, BBR-M-10 diminished metastatic phenotypes, including reduced EMT and sialylation. The AKT pathway may potentially serve a vital role in this inhibitory effect. These findings suggested that BBR-M-10 could potentially be used in the future as a treatment for metastatic CCA.

Acknowledgements

We thank Mr. Bryan Roderick Hamman, Publication Clinic, Research Affairs, Faculty of Medicine, Khon Kaen University, Khon Kaen 40002, Thailand for assistance with the English language editing of the manuscript. We thank Professor Sopit Wongkham, Department of Biochemistry, Faculty of Medicine, Khon Kaen University, Khon Kaen 40002, Thailand for providing the immortalized human cholangiocyte MMNK-1 cell line.

Funding

The present work was supported by the Thailand Research Fund International Research Network grant (grant no. IRN62W0004) and both the Suranaree University of Technology, Thailand Science Research and Innovation (TSRI) and National Science, Research and Innovation Fund (grant no. 179281).

Availability of data and materials

The data generated in the present study may be requested from the corresponding author.

Authors' contributions

JKC, CT and KT acquired grant resources. CT conceived and designed the study. SK, SC and CT performed the experiments. CT and SK analyzed the data. JKC and KT provided advice and resources. SK drafted the manuscript. CT and JKC revised the manuscript. JKC assisted with English language editing. All authors have read and approved the final version of the manuscript. CT and SK confirm the authenticity of all the raw data.

Ethics approval and consent to participate

Not applicable.

Patient consent for publication

Not applicable.

Competing interests

The authors declare that they have no competing interests.

References

1. Tan BL, Norhaizan ME and Chan LC: Rice bran: From waste to nutritious food ingredients. Nutrients 15: 2503, 2023.
2. Wisetkomolmat J, Arjin C, Satsook A, Seel-Audom M, Ruksiriwanich W, Prom UTC and Sringarm K: Comparative analysis of nutritional components and phytochemical attributes of selected Thai rice bran. Front Nutr 9: 833730, 2022.
3. Manzoor A, Kumar Pandey V, Dar AH, Fayaz U, Dash KK, Shams R, Ahmad S, Bashir I, Fayaz J, Singh P, *et al*: Rice bran: Nutritional, phytochemical, and pharmacological profile and its contribution to human health promotion. Food Chem Adv 2: 100296, 2023.
4. Gonçalves AC, Nunes AR, Falcão A, Alves G and Silva LR: Dietary effects of anthocyanins in human health: a comprehensive review. Pharmaceuticals (Basel) 14: 690, 2021.
5. Khoo HE, Azlan A, Tang ST and Lim SM: Anthocyanidins and anthocyanins: Colored pigments as food, pharmaceutical ingredients, and the potential health benefits. Food Nutr Res 61: 1361779, 2017.
6. de Sousa Moraes LF, Sun X, Peluzio MDCG and Zhu MJ: Anthocyanins/anthocyanidins and colorectal cancer: What is behind the scenes? Crit Rev Food Sci Nutr 59: 59-71, 2019.

7. Khophai S, Chokchaisiri S, Talabnin K, Ketudat Cairns JR and Talabnin C: Black rice bran-derived anthocyanins prevent H2O2-induced oxidative stress and DNA damage in cholangiocytes through activation of the Nrf2-NQO1 axis. ScienceAsia (In press).
8. Joshua M, Okere C, Sylvester O, Yahaya M, Precious O, Dluya T, Um JY, Neksumi M, Boyd J, Vincent-Tyndall J, *et al*: Disruption of angiogenesis by anthocyanin-rich extracts of Hibiscus sabdariffa. Int J Sci Eng Res 8: 299-307, 2017.
9. Wang L, Zhou P, Feng R, Luo Z, Li X and Gao L: Anti-proliferation activities of *Oryza sativa* L. anthocyanins-Hohenbuehelia serotina polysaccharides complex after in vitro gastrointestinal digestion. Food Chem Toxicol 135: 111012, 2020.
10. Chen PN, Kuo WH, Chiang CL, Chiou HL, Hsieh YS and Chu SC: Black rice anthocyanins inhibit cancer cells invasion via repressions of MMPs and u-PA expression. Chem Biol Interact 163: 218-229, 2006.
11. Sun W, Zhang ND, Zhang T, Li YN, Xue H, Cao JL, Hou WS, Liu J, Wang Y and Jin CH: Cyanidin-3-O-glucoside induces the apoptosis of human gastric cancer MKN-45 cells through ROS-mediated signaling pathways. Molecules 28: 652, 2023.
12. Lee J, Shin A, Oh JH and Kim J: Colors of vegetables and fruits and the risks of colorectal cancer. World J Gastroenterol 23: 2527-2538, 2017.
13. Xu C, Zeng XT, Liu TZ, Zhang C, Yang ZH, Li S and Chen XY: Fruits and vegetables intake and risk of bladder cancer: A PRISMA-compliant systematic review and dose-response meta-analysis of prospective cohort studies. Medicine (Baltimore) 94: e759, 2015.
14. Larsson SC, Bergkvist L and Wolk A: Fruit and vegetable consumption and incidence of gastric cancer: A prospective study. Cancer Epidemiol Biomarkers Prev 15: 1998-2001, 2006.
15. Srivatanakul P, Sriplung H and Deerasamee S: Epidemiology of liver cancer: An overview. Asian Pac J Cancer Prev 5: 118-125, 2004.
16. Sripa B and Pairojkul C: Cholangiocarcinoma: Lessons from Thailand. Curr Opin Gastroenterol 24: 349-356, 2008.
17. Sarcognato S, Sacchi D, Fassan M, Fabris L, Cadamuro M, Zanus G, Cataldo I, Capelli P, Baciorri F, Cacciatore M and Guido M: Cholangiocarcinoma. Pathologica 113: 158-169, 2021.
18. van Tienderen GS, van Beek MEA, Schurink IJ, Rosmark O, Roest HP, Tieleman J, Demmers J, Muntz I, Conboy J, Westergren-Thorsson G, *et al*: Modelling metastatic colonization of cholangiocarcinoma organoids in decellularized lung and lymph nodes. Front Oncol 12: 1101901, 2023.
19. Intuyod K, Priprem A, Limphirat W, Charoensuk L, Pinlaor P, Pairojkul C, Lertrat K and Pinlaor S: Anti-inflammatory and anti-periductal fibrosis effects of an anthocyanin complex in *Opisthorchis viverrini*-infected hamsters. Food Chem Toxicol 74: 206-215, 2014.
20. Intuyod K, Priprem A, Pairojkul C, Hahnvajanawong C, Vaeteewoottacharn K, Pinlaor P and Pinlaor S: Anthocyanin complex exerts anti-cholangiocarcinoma activities and improves the efficacy of drug treatment in a gemcitabine-resistant cell line. Int J Oncol 52: 1715-1726, 2018.
21. Sripa B, Seubwai W, Vaeteewoottacharn K, Sawanyawisuth K, Silsirivanit A, Kaewkong W, Muisuk K, Dana P, Phoomak C, Lert-Itthiporn W, *et al*: Functional and genetic characterization of three cell lines derived from a single tumor of an *Opisthorchis viverrini*-associated cholangiocarcinoma patient. Hum Cell 33: 695-708, 2020.
22. Pangestu NS, Chueakwon P, Talabnin K, Khiaowichit J and Talabnin C: RNF43 overexpression attenuates the Wnt/β-catenin signalling pathway to suppress tumour progression in cholangiocarcinoma. Oncol Lett 22: 846, 2021.
23. Talabnin C, Trasaktaweesakul T, Jaturutthaweechot P, Asavaritikrai P, Kongnawakun D, Silsirivanit A, Araki N and Talabnin K: Altered O-linked glycosylation in benign and malignant meningiomas. PeerJ 12: e16785, 2024.
24. Livak KJ and Schmittgen TD: Analysis of relative gene expression data using real-time quantitative PCR and the 2(-Delta Delta C(T)) method. Methods 25: 402-408, 2001.
25. Nichols WW, Cristofalo VJ, Toji LH, Greene AE, Aronson MM, Dwight S, Charpentier R and Hoffman E: Characterization of a new human diploid cell line-IMR-91. In Vitro 19: 797-804, 1983.
26. Izdebska M, Zielińska W, Grzanka D and Gagat M: The role of actin dynamics and actin-binding proteins expression in epithelial-to-mesenchymal transition and its association with cancer progression and evaluation of possible therapeutic targets. Biomed Res Int 2018: 4578373, 2018.
27. Karimi Roshan M, Soltani A, Soleimani A, Rezaie Kahkhaie K, Afshari AR and Soukhtanloo M: Role of AKT and mTOR signaling pathways in the induction of epithelial-mesenchymal transition (EMT) process. Biochimie 165: 229-234, 2019.
28. Lucena MC, Carvalho-Cruz P, Donadio JL, Oliveira IA, de Queiroz RM, Marinho-Carvalho MM, Sola-Penna M, de Paula IF, Gondim KC, McComb ME, *et al*: Epithelial mesenchymal transition induces aberrant glycosylation through hexosamine biosynthetic pathway activation. J Biol Chem 291: 12917-12929, 2016.
29. Brown JS, Amend SR, Austin RH, Gatenby RA, Hammarlund EU and Pienta KJ: Updating the definition of cancer. Mol Cancer Res 21: 1142-1147, 2023.
30. Anderson RL, Balasas T, Callaghan J, Coombes RC, Evans J, Hall JA, Kinrade S, Jones D, Jones PS, Jones R, *et al*: A framework for the development of effective anti-metastatic agents. Nat Rev Clin Oncol 16: 185-204, 2019.
31. Chansitthichok S, Chamnan P, Sarkhampee P, Lertsawatvicha N, Voravisutthikul P and Wattanarath P: Survival of patients with cholangiocarcinoma receiving surgical treatment in an *O. viverrini* endemic area in Thailand: A retrospective cohort study. Asian Pac J Cancer Prev 21: 903-909, 2020.
32. Sarkhampee P, Ouransatien W, Lertsawatvicha N, Chansitthichok S and Wattanarath P: Survival outcome of 736 cholangiocarcinoma patient receiving surgical treatment in Thailand. HPB 25 (Suppl 2): S265-S266, 2023.
33. Zhou J, Zhu YF, Chen XY, Han B, Li F, Chen JY, Peng XL, Luo LP, Chen W and Yu XP: Black rice-derived anthocyanins inhibit HER-2-positive breast cancer epithelial-mesenchymal transition-mediated metastasis *in vitro* by suppressing FAK signaling. Int J Mol Med 40: 1649-1656, 2017.
34. Jongsomchai K, Leardkamolkarn V and Mahatheeranont S: A rice bran phytochemical, cyanidin 3-glucoside, inhibits the progression of PC3 prostate cancer cell. Anat Cell Biol 53: 481-492, 2020.
35. Maruyama M, Kobayashi N, Westerman KA, Sakaguchi M, Allain JE, Totsugawa T, Okitsu T, Fukazawa T, Weber A, Stolz DB, *et al*: Establishment of a highly differentiated immortalized human cholangiocyte cell line with SV40T and hTERT. Transplantation 77: 446-451, 2004.
36. Prakobwong S, Gupta SC, Kim JH, Sung B, Pinlaor P, Hiraku Y, Wongkham S, Sripa B, Pinlaor S and Aggarwal BB: Curcumin suppresses proliferation and induces apoptosis in human biliary cancer cells through modulation of multiple cell signaling pathways. Carcinogenesis 32: 1372-1380, 2011.
37. Wu A, Zhu Y, Han B, Peng J, Deng X, Chen W, Du J, Ou Y, Peng X and Yu X: Delphinidin induces cell cycle arrest and apoptosis in HER-2 positive breast cancer cell lines by regulating the NF-κB and MAPK signaling pathways. Oncol Lett 22: 832, 2021.
38. Huang Y, Hong W and Wei X: The molecular mechanisms and therapeutic strategies of EMT in tumor progression and metastasis. J Hematol Oncol 15: 129, 2022.
39. Lai X, Li Q, Wu F, Lin J, Chen J, Zheng H and Guo L: Epithelial-mesenchymal transition and metabolic switching in cancer: Lessons from somatic cell reprogramming. Front Cell Dev Biol 8: 760, 2020.
40. Lamouille S, Xu J and Derynck R: Molecular mechanisms of epithelial-mesenchymal transition. Nat Rev Mol Cell Biol 15: 178-196, 2014.
41. Lorente G, Syriani E and Morales M: Actin filaments at the leading edge of cancer cells are characterized by a high mobile fraction and turnover regulation by profilin I. PLoS One 9: e85817, 2014.
42. Chen M, Zhu W, Liang Z, Yao S, Zhang X and Zheng Y: Effect of f-actin organization in lamellipodium on viscoelasticity and migration of Huh-7 cells under pH microenvironments using AM-FM atomic force microscopy. Front Phys 9: 674958, 2021.
43. Chung WL, Eibauer M, Li W, Boujemaa-Paterski R, Geiger B and Medalia O: A network of mixed actin polarity in the leading edge of spreading cells. Commun Biol 5: 1338, 2022.
44. Olson MF and Sahai E: The actin cytoskeleton in cancer cell motility. Clin Exp Metastasis 26: 273-287, 2009.
45. Lee EJ, Kang MK, Kim YH, Kim DY, Oh H, Kim SI, Oh SY and Kang YH: Dietary chrysin suppresses formation of actin cytoskeleton and focal adhesion in AGE-exposed mesangial cells and diabetic kidney: Role of autophagy. Nutrients 11: 127, 2019.
46. Berr AL, Wiese K, Dos Santos G, Koch CM, Anekalla KR, Kidd M, Davis JM, Cheng Y, Hu YS and Ridge KM: Vimentin is required for tumor progression and metastasis in a mouse model of non-small cell lung cancer. Oncogene 42: 2074-2087, 2023.

47. Usman S, Waseem NH, Nguyen TKN, Mohsin S, Jamal A, Teh MT and Waseem A: Vimentin is at the heart of epithelial mesenchymal transition (EMT) mediated metastasis. Cancers (Basel) 13: 4985, 2021.
48. Rao RK and Samak G: Bile duct epithelial tight junctions and barrier function. Tissue Barriers 1: e25718, 2013.
49. Bhat AA, Syed N, Therachiyil L, Nisar S, Hashem S, Macha MA, Yadav SK, Krishnankutty R, Muralitharan S, Al-Naemi H, *et al*: Claudin-1, A double-edged sword in cancer. Int J Mol Sci 21: 569, 2020.
50. Maharati A and Moghbeli M: PI3K/AKT signaling pathway as a critical regulator of epithelial-mesenchymal transition in colorectal tumor cells. Cell Commun Signal 21: 201, 2023.
51. Yothaisong S, Dokduang H, Techasen A, Namwat N, Yongvanit P, Bhudhisawasdi V, Puapairoj A, Riggins GJ and Loilome W: Increased activation of PI3K/AKT signaling pathway is associated with cholangiocarcinoma metastasis and PI3K/mTOR inhibition presents a possible therapeutic strategy. Tumour Biol 34: 3637-3648, 2013.
52. Vaquero J, Guedj N, Clapéron A, Nguyen Ho-Bouldoires TH, Paradis V and Fouassier L: Epithelial-mesenchymal transition in cholangiocarcinoma: From clinical evidence to regulatory networks. J Hepatol 66: 424-441, 2017.
53. Suman S, Kurisetty V, Das TP, Vadodkar A, Ramos G, Lakshmanaswamy R and Damodaran C: Activation of AKT signaling promotes epithelial-mesenchymal transition and tumor growth in colorectal cancer cells. Mol Carcinog 53 (Suppl 1): E151-E160, 2014.
54. Moghbeli M: PI3K/AKT pathway as a pivotal regulator of epithelial-mesenchymal transition in lung tumor cells. Cancer Cell Int 24: 165, 2024.
55. Chen W, Wu S, Zhang G, Wang W and Shi Y: Effect of AKT inhibition on epithelial-mesenchymal transition and ZEB1-potentiated radiotherapy in nasopharyngeal carcinoma. Oncol Lett 6: 1234-1240, 2013.
56. Lee S, Choi EJ, Cho EJ, Lee YB, Lee JH, Yu SJ, Yoon JH and Kim YJ: Inhibition of PI3K/Akt signaling suppresses epithelial-to-mesenchymal transition in hepatocellular carcinoma through the Snail/GSK-3/beta-catenin pathway. Clin Mol Hepatol 26: 529-539, 2020.
57. Layosa MAA, Lage NN, Chew BP, Atienza L, Mertens-Talcott S, Talcott S and Noratto GD: Dark sweet cherry (Prunus avium) phenolics enriched in anthocyanins induced apoptosis in MDA-MB-453 breast cancer cells through MAPK-dependent signaling and reduced invasion via Akt and PLCγ-1 downregulation. Nutr Cancer 73: 1985-1997, 2021.
58. Zhong W, Tong Y, Li Y, Yuan J, Hu S, Hu T and Song G: Mesenchymal stem cells in inflammatory microenvironment potently promote metastatic growth of cholangiocarcinoma via activating Akt/NF-κB signaling by paracrine CCL5. Oncotarget 8: 73693-73704, 2017.
59. Chen XY, Zhou J, Luo LP, Han B, Li F, Chen JY, Zhu YF, Chen W and Yu XP: Black rice anthocyanins suppress metastasis of breast cancer cells by targeting RAS/RAF/MAPK pathway. Biomed Res Int 2015: 414250, 2015.
60. Gabius HJ: The sugar code: Why glycans are so important. Biosystems 164: 102-111, 2018.
61. Pucci M, Malagolini N and Dall'Olio F: Glycobiology of the epithelial to mesenchymal transition. Biomedicines 9: 770, 2021.
62. Park DD, Xu G, Park SS, Haigh NE, Phoomak C, Wongkham S, Maverakis E and Lebrilla CB: Combined analysis of secreted proteins and glycosylation identifies prognostic features in cholangiocarcinoma. J Cell Physiol 239: e31147, 2024.
63. Lu J, Isaji T, Im S, Fukuda T, Hashii N, Takakura D, Kawasaki N and Gu J: β-Galactoside α2,6-sialyltranferase 1 promotes transforming growth factor-β-mediated epithelial-mesenchymal transition. J Biol Chem 289: 34627-34641, 2014.

Copyright © 2024 Khophai et al. This work is licensed under a Creative Commons Attribution-NonCommercial-NoDerivatives 4.0 International (CC BY-NC-ND 4.0) License.